Concentric circles based simple optical landing aid for vertical takeoff and landing aircrafts

Syed H. Murshid[1,2,3], Rayan Enaya[1,2,3], and Gregory L. Lovell[1,2,3]
[1]SPIE Member
[2]Optronics Laboratory
[3]Department of Electrical and Computer Engineering, Florida Institute of Technology
150 West University Boulevard, Melbourne, FL 32901
murshid@ee.fit.edu, renaya@my.fit.edu, glovell@my.fit.edu

ABSTRACT

Vertical takeoff and landing (VTOL) aircrafts such as helicopters and drones, add a flexible degree of operation to airborne vehicles. In order to operate these devices in low light situations, where it is difficult to determine slope of the landing surface, a lightweight and standalone device is proposed here. This small optical device can be easily integrated into current VTOL systems. An optical projector consisting of low power, light weight, solid state laser along with minimal optics is utilized to illuminate the landing surface with donut shaped circles and coaxial centralized dot. This device can placed anywhere on the aircraft and a properly placed fiber system can be used to illuminate the surface beneath the bottom of the VTOL aircraft in a fashion that during operation, when the aircraft is parallel to the landing surface, the radius between the central dot and outer ring(s) are equidistant for the entire circumference; however, when there the landing surface of the VTOL aircraft is not parallel to the landing strip, the radial distance between two opposite sides of the circle and central dot will be unequal. The larger this distortion, the greater the difference will be between the opposite sides of the circle. Visual confirmation or other optical devices can be used to determine relative alignment of the projector output allowing the pilot to make proper adjustments as they approach the landing surface to ensure safe landings. Simulated and experimental results from a prototype optical projector are presented here.

Keywords: VTOL, Visual Landing Aid, fiber optics,

1. INTRODUCTION

Vertical take-off and landing (VTOL) aircrafts refer to those that have the ability to take off or land vertically, such as helicopters, sea harriers, and certain UAVs. Landing these aircrafts could be a challenge during non-ideal conditions, such as brown-outs, and it may render these platforms dangerous to operate[1,2]. Situations such as sandy or snowy slopes under a blizzard or sand storm, or on ships during inclement weather, where the landing surface is pitching or shifting constantly, offer considerable challenge to the aircraft and its pilots. Research into predicting this motion has been ongoing for many decades now[3-7]; however, no amount of prediction or calculations can account for sudden changes in weather or irregularities in the VTOL's behavior. Various alternative approaches have been developed to assist with the landing process such as the standard visual landing aids (VLAs)[8], flight deck lighting[9-11], landing period designators (LPD)[12-16], Fresnel lens OLS[17-19], ICOLS[20,21], and virtual imaging systems for approach and landing (VISUAL)[22-24]. These systems require either visual cues from personnel or situational lighting which makes factors such as pilot decisions more relevant[25,26]. Even with these approaches in place, accidents still occur. Other more extreme situations, such as the sandy slopes, carry even higher degrees of difficulty as the blades of standard current VTOL aircraft will produce a localized storm in the vicinity of aircraft and significantly reduce visibility. This also has the potential to shift the landing surface considerably, throwing all earlier calculations/predictions unreliable.

This endeavor proposes a low power, low cost, light weight, and standalone visual landing aid to composed of a simple optical projector to combat these and similar issues. The proposed optical projector can be easily integrated into existing VTOL aircrafts. The optical projector can be designed in a multitude of ways such as a low power, low cost solid state laser that is coupled to a small length of optical fiber in a fashion that it illuminates the landing surface with a donut shaped ring and a centralized coaxial dot. The output end of the projector system can be attached to a horizontal surface

Photonics Applications for Aviation, Aerospace, Commercial, and Harsh Environments V,
edited by Alex A. Kazemi, et. al., Proc. of SPIE Vol. 9202, 920218 · © 2014 SPIE
CCC code: 0277-786X/14/$18 · doi: 10.1117/12.2075231

along the bottom of the VTOL aircraft that is aligned to be parallel to the landing gear. The rest of the projector system could be at any desired location on the aircraft. To ensure that the aircraft is properly aligned and parallel to the landing surface, the central dot from the projector is should be radially equidistant to the donut shaped outer ring; however, if the landing surface is not properly aligned, the circle will be distorted with asymmetrical distances between the coaxial dot and the outer ring. The greater this distortion in the illuminated pattern, the greater is the incline on the landing surface. By analyzing this distortion, one can determine the shape of the landing surface. The pilot could use visual cues or an onboard camera based system to analyze the landing surface topology. In this manner, the analysis can be completely done via an onboard computer to provide quick and precise data in real time; furthermore, different wavelengths of light can be utilized in order to allow the optical ring structure to penetrate dust, snow or other debris/particulates surrounding the landing zone. Figure 1 graphically depicts the operation of the proposed device.

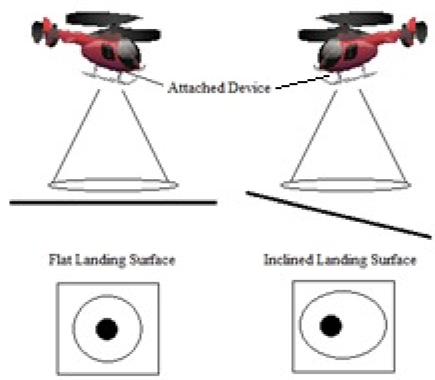

Figure 1: Graphic representation of the proposed landing aid. On a flat surface when the VTOL is aligned, the output signal appears exactly the same as an input signal; however, in case of an inclined surface or unaligned VTOL, the output will assume an elliptical shape with unequal distances between the central spot and complementary edges of the projected circle.

Analysis of this design through modelling, Optical Software for Layout and Optimization (OSLO)[27] based simulation software and experimental means are performed to verify the suitability of the system design. The simulated and experimental data is then compared to theoretical data of the model.

2. SIMULATION MODEL

In order to analyze the proposed design, OSLO optical simulation software engine was used. Since the proposed optical projector uses a combination of two or more concentric rings or concentric center spot and a ring, a very simple design similar to an axicon lens, with a small aperture, was used to generate a concentric dot and ring combo in OSLO. The simulated wireframe design as well as the output spot diagram can be seen in figure 2. This lens converts incoming beams of light into desired concentric ring pattern.

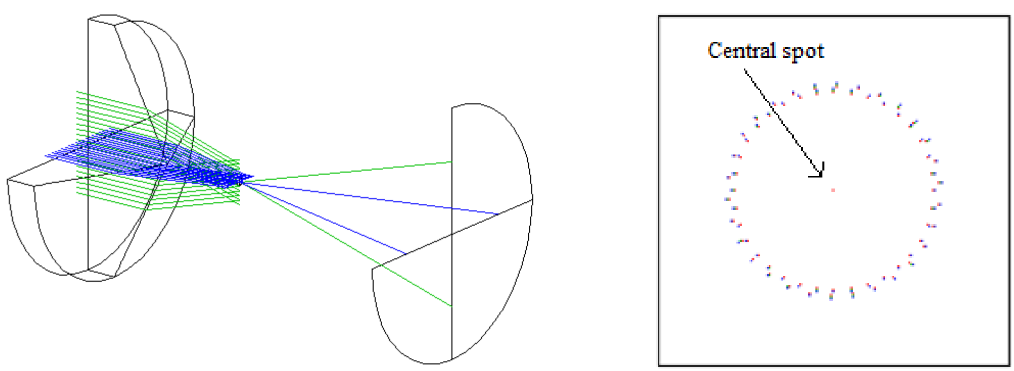

Figure 2: An axicon lens simulates the desired optical pattern. A small aperture limits generated rings to two. The image on the left shows the lens setup while that on the right shows spot diagram for zero degree rotated image plane, simulating a flat landing surface.

Once the output pattern is generated, the image plane can be inclined in various fashions to simulate different landing surfaces. In order to properly compare each scenario, a set of axes were drawn on each image, where the central dot is set at the vertices of these axes. The simulated results with added axes are presented in figure 3. These images were taken with a screen rotation in the clockwise direction along the y-axis.

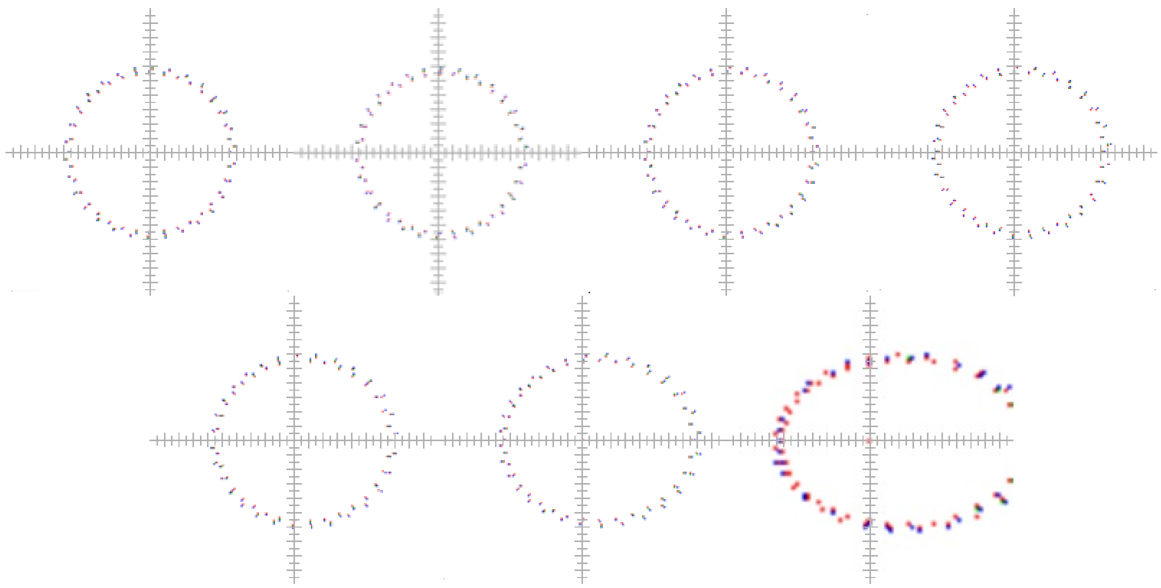

Figure 3: Simulated ring pattern using the spot diagram function in OSLO. The ring pattern is displayed by rotating the image surface in the clockwise direction. The patterns results for following angles are presented from top left to bottom right: 0^0, 5^0, 10^0, 15^0, 20^0, 30^0, and 45^0. The central dot for all patterns is located at the vertices of the axes.

As shown in figure 4, similar results are obtained by varying the orientation of the image plane in alternative directions. These results show that the design will work for various surface inclinations and in all directions.

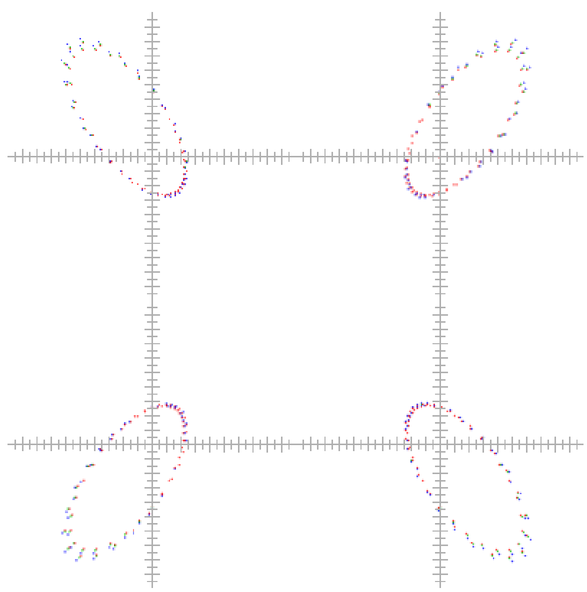

Figure 4: Results from OSLO simulation. All angles presented are for 45 degrees; however with different rotations of the x and y axes. Top-left: counter clockwise (CCW)-X, CCW-Y. Top-Right: CCW-X, Clockwise (CW)-Y. Bottom-Left: CW-X, CCW-Y. Bottom-Right: CW-X, CW-Y. Note that this image is on a slightly different scale than figure 3.

3. EXPERIMENTAL VERIFICATION OF THE DESIGN

Experimental verification of the design was achieved using an inexpensive fiber optic coaxial ring projection system that was initially developed for a novel optical multiplexing technique called spatial domain multiplexing (SDM)[28-35]. The application of SDM techniques add two new degrees of photon freedom to optical fiber systems. In short SDM is a multiple input multiple output (MIMO) system that allows generation of multiple rings (or central spot and rings) by utilizing multiple sources and varying the input launch angle at which they couple to a particular optical fiber. As the sources traverse the carrier fiber, they follow helical trajectories and form concentric rings as the output of the carrier fiber is projected on a screen owing to presence of optical vortices[36,37]. A two channel SDM system was used to generate a central spot and a concentric outer ring to experimentally verify the proposed design.

The experimental data was analyzed using two different but effectively similar methods. The first method analyzed the screen projection of the output directly while the second method utilized a software script to develop intensity graphs for subsequent analysis. The results from the first method are presented in figure 5. These results were taken in a manner similar to the OSLO simulation. The projection screen is rotated in a CW direction ranging from zero to forty five degrees to simulate different landing scenarios.

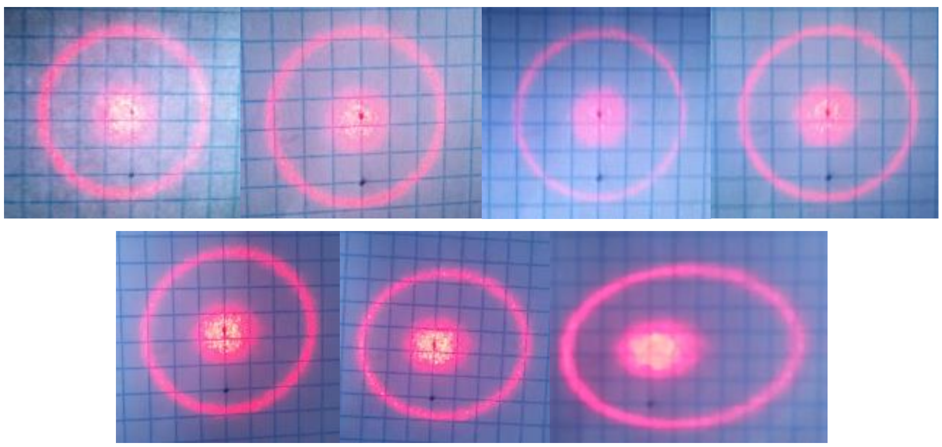

Figure 5: Experimental data using SDM method of generating rings. The screen is rotated in a clockwise direction. The angles are as follows going from the top left image to the bottom right image: 0^0, 5^0, 10^0, 15^0, 20^0, 30^0, and 45^0.

As the screen is rotated, the right side of the secondary ring becomes elongated over time. While the difference is small for lower angles, it is highly noticeable at higher angles, where landing a VTOL aircraft could be dangerous. To better analyze these results, intensity graphs of simulated rings with very similar projector to screen orientations were created and then the screen was rotated in a clockwise direction between 0^0 - 45^0. Figure 6 depicts these results.

As with the prior results, less challenging misalignments caused by lower angles, though discernible, did not raise any unnecessary visual flags; however, the intensity plots for larger angular misalignments show differences that just cannot be missed even by the naked eye. As a result this system should be of significant assistance to pilots attempting to land in difficult situations. In the experimental setup, the central dot is large compared to the simulated data. As a result the distortion due to angular misalignment between the two surfaces is noticeable in both the outer ring as well as the central spot, albeit to different degrees. The spot becomes more elliptical as the screen angle is increased. This causes the intensity plots to show a much broader central region at higher angles. The effect is most noticeable for angles exceeding 15^0 where notable plateau regions of lower intensity are formed on the side of the central region.

The outside ellipse offers two noteworthy observations. The central point of the right side of the intensity plots moves farther from the central region as the inclination increases. This is easily noticed by the fact that the axis is slowly increasing between the graphs. Secondly the intensity of the second peak starts to very quickly taper off. As a result algorithms could be developed that generate thresholds to assist with automated abort/land decisions.

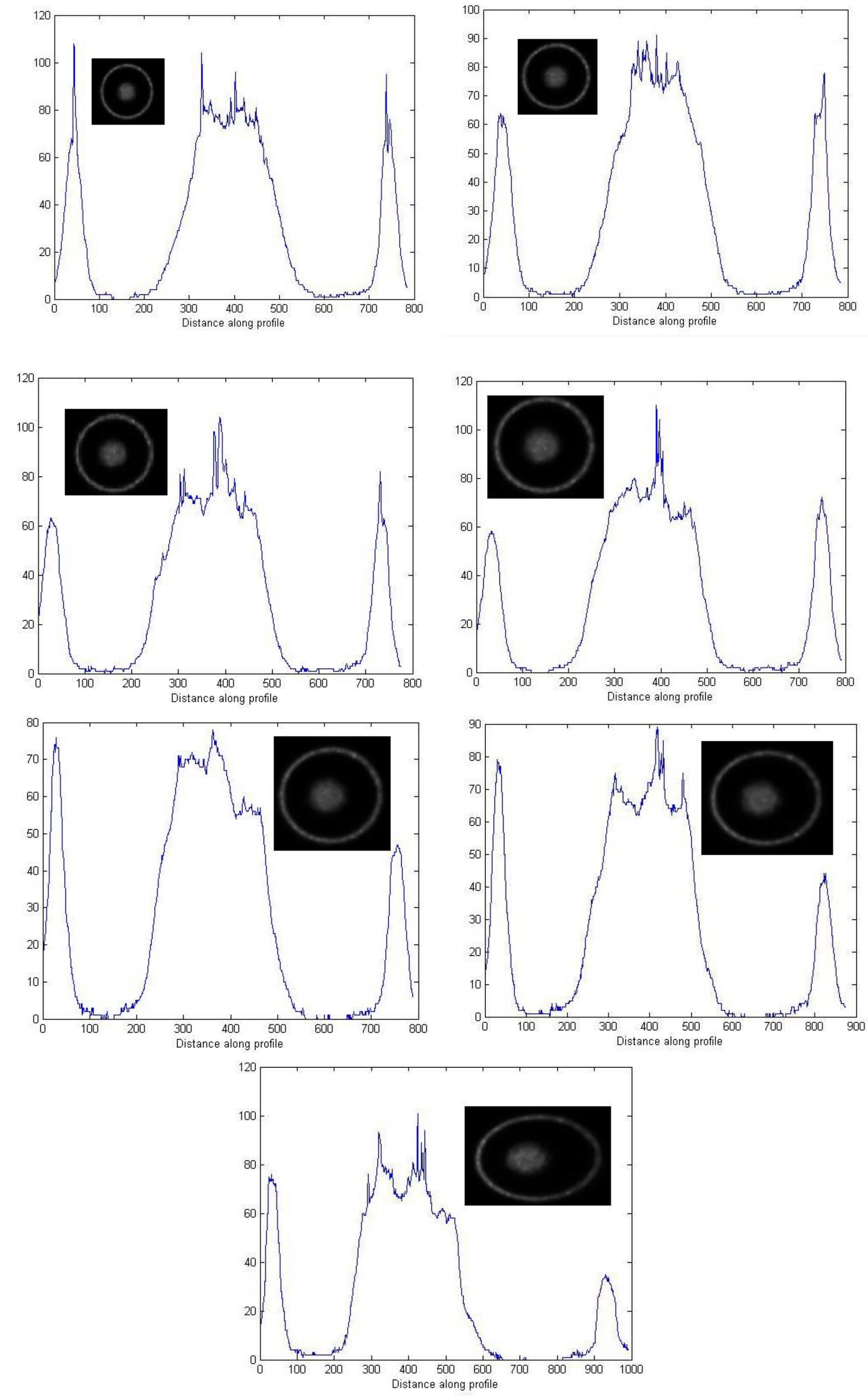

Figure 6: Intensity profiles for experimental data. Angles of rotation are as follows starting from top left to the bottom graph: 0^0, 5^0, 10^0, 15^0, 20^0, 30^0, and 45^0.

4. THEORETICAL RESULTS ANALYSIS AND COMPARISONS

4.1 Theoretical Model and Equation

To better analyze the results from the experimental and simulated models, a theoretical model and equation was formulated. The model compares the distance between the most distorted sections of the outer ring and the opposite side.

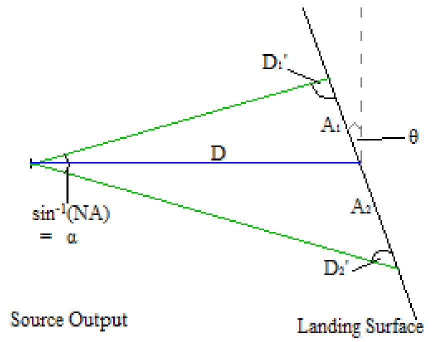

Figure 7: Theoretical model of the output of the proposed device. The rings leaving the device will spread as a function of the fiber's numerical aperture. The θ term is the incline of the landing surface.

As shown in figure 7, one can use the Sine law along with trigonometric identities to develop an equation describing this relationship. Equation 1 shows the initial setup of the model while equation 2 presents the final results as a function of the ratio of A_1/A_2.

$$\frac{\sin(\alpha)}{A_{1,2}} = \frac{\sin(D'_{1,2})}{D} \quad (1)$$

$$\frac{A_1}{A_2} = \cos(2\theta) - \cot(D'_1)\sin(2\theta) \quad (2)$$

where A_1 and A_2 are the lengths of the shortest and longest sides of the rings respectively, θ is the inclination of the landing surface, and D_1' is the angle opposite of the center spot, D, represents the vertical distance between the VTOL is from the landing surface while D_1 and D_2 are the angles related to the landing surface and the term D_1' can be found using equation 3.

$$D'_1 = 90 + \theta - \alpha/2 \quad (3)$$

where α is angle of the incident cone due to the numerical aperture (NA) of the utilized fiber.

4.2 Results and Comparisons to Theoretical Model

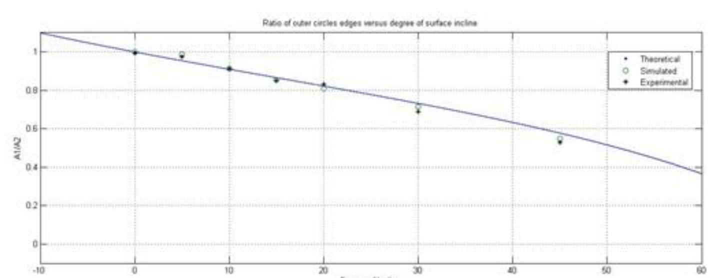

Figure 8: Data comparison between mathematical (theoretical), simulated, and an average of the experimental models.

Figure 8 contains the recorded data for the proposed design for each of the three stages. The theoretical data is a plot of the ratio in equation 3. The simulated data is gathered by taking the ratio of the left edge to the right edge distances in figure 3. The experimental data is gathered by taking the average of several methods ranging from counting the squares and taking the ratio in figure 5 to measuring several points along the intensity graphs in figure 6. The three sets of data depict a strong correlation to one another which acts to show the validity of the proposed optical landing aid design.

5. CONCLUSION

VTOL operation is often dependent upon landing scenarios. In order to minimize the challenges associated with this process, an architecture is proposed that will allow pilots to make adjustments to their orientation based upon the inclination of the landing surface in real time by utilizing an optical projector that produces a concentric central dot and an outer donut shaped ring. Elliptical shifts in circular geometry of the ring suggests misalignments that could be easily utilized as readily available airborne optical cues and can also be measured and relayed back to the pilots. Results presented show good correlation between the theoretical, simulated and experimental results. Further analysis and computational additions can allow onboard analysis of slope of the landing surface, distance between and topography of varying contours, such as bowl shaped landing surfaces often encountered in sand dunes and snowy slopes. This technique may also be used for 3-D mapping of a broad range of surfaces.

6. REFERENCES

[1] Berbaum, K. S., R. S. Kennedy, et al. (1991). "Visual Tasks in Helicopter Shipboard Landing." Applied Ergonomics 22(4): 231-239.

[2] Garnett, T. S. J. and J. M. Davis (1977). The Helicopter/Ship Dynamic-Interface Problem. Navy/NASA V/STOL Flying Qualities Workshop. Monterey, CA.

[3] Fleischmann, D. S. (2000). Method and System for Predicting Ship Motion or the Like to Assist in Helicopter Landing. U. S. P. Office. USA, Lockheed Martin Corporation. 6064924.

[4] Kaplan, P. (1969). "A Study of Prediction Techniques for Aircraft Carrier Motions at Sea." Journal of Hydronautics 3(3): 121-131.

[5] Colwell, J. L. (2004). Flight Deck Motion System (FDMS): Operating Concepts and System Description. D. o. D. R. a. D. Canada, DRDC Atlantic.

[6] Sherman, Brook W. "Thesis(complete)v4 : LIB 05092007 : Virginia Tech."Thesis(complete)v4 : LIB 05092007 : Virginia Tech. Virginia Polytechnic Institute and State University, n.d.

[7] Advani, S. K. D. and C. H. Wilkinson (2001). Dynamic Interface Modelling and Simulation - A Unique Challenge. Helicopter Flight Simulation Conference. London, England, Royal Aeronautical Society

[8] Langlois, R. G., M. LaRosa, et al. (2003). Development, Validation, and Application of the Dynaface Helicopter/Ship Dynamic Interface Simulation Software Package. Summer Computer Simulation Conference, Montreal, Canada, Society for Modeling and Simulation International (SCS).

[9] Carico, D. and C. Slade., Fiber Optic Ship Flight Deck Lighting for the New Millennium, SFTE Symposium 31, Turin, Italy, September 2000.

[10] SAE-AS25050, Colors, Aeronautical Lights and Lighting Equipment, General Requirements For, September 13 1999.

[11] Smith, Anthony, The Design of Visual Landing Aids for Shipborne Helicopters, ASNE Day 2001, Washington, D.C., April 2001.

[12] Ferrier, B., A. E. Baitis, et al. (2000). "Evolution of the Landing Period Designator (LPD) for Shipboard Air Operations." Naval Engineers Journal 112(4): 297-315.

[13] Ferrier, B. and T. Manning (1998). "Simulation and Testing of the Landing Period Designator (LPD) Helicopter Recovery Aid." Naval Engineers Journal 110(1): 189-205.

[14] Carico, D. and B. Ferrier (2006). Evaluating Landing Aids to Support Helicopter/Ship Testing and Operations. IEEE Aerospace Conference, IEEE.

[15] Ferrier, B. (1998). Experiences with the Landing Period Designator (LPD) Helicopter Recovery Aid in High Sea States. 54th Forum of the American Helicopter Society. Washington, DC, American Helicopter Society.

[16] Ferrier, B., T. Applebee, et al. (2000). Landing Period Designator Visual Helicopter Recovery Aide; Theory and Real-Time Application. Proceedings of the American Helicopter Society, Washington.

[17] Barthelme, Richard W., John N. Biercuk, and John B. Leonard. "Ship compatible launch, retrieval and handling system for (VTOL) aircraft." U.S. Patent No. 4,236,686. 2 Dec. 1980.

[18] "HELICOPTER OTPICAL POSITION INDICATOR." U.S. Patent 3,843,263, issued October 22, 1974.

[19] Fitzgerald, Pio. "Flight control system design for autonomous UAV carrier landing." (2004).

[20] Prickett, Arthur, "Analysis of the Instrument Carrier Landing System Certification Process for Amphibious Assault Ships. " Master's Thesis, University of Tennessee, 2003.

[21] ZHENG, Feng-ying, and Yi-dong YANG. "Research on Longitudinal Landing Precision for Carrier-Based Aircraft Based on “ICOLS” Laser Aided Landing System." Command Control & Simulation 2 (2007): 028.

[22] Hamel, Tarek, and Robert Mahony. "Visual servoing of an under-actuated dynamic rigid-body system: an image-based approach." Robotics and Automation, IEEE Transactions on 18.2 (2002): 187-198.

[23] Ferren, Bran, W. Daniel Hillis, and Michael Harvey Peterson. "Imaging and display system to aid helicopter landings in brownout conditions." U.S. Patent No. 8,019,490. 13 Sep. 2011.

[24] Frietsch, Natalie, et al. "Vision based hovering and landing system for a VTOL-MAV with geo-localization capabilities." AIAA Guidance, Navigation and Control Conference and Exhibit. 2008.

[25] Allender, L. (2000). Modeling Human Performance: Impacting System Design, Performance, and Cost. Military, Government and Aerospace Simulation Symposium, 2000 Advanced Simulation Technologies Conference, Washington D. C.

[26] Descleves, E. (2007). "A Step Forward in At-Sea Decision-Making." U.S. Naval Institute Proceedings 133/2/1248(February): 68-69.

[27] Lambda Research Corporation, OSLO: Optics Software for Layout and Optimization: Optics Reference (2005).

[28] S. H. Murshid, B. Grossman, and P. Narakorn. “Spatial Domain Multiplexing: a new dimension in fiber optic multiplexing”, Journal of Optics and Laser Technology, 40(8), 1030-1036, (2008).

[29] S. H. Murshid, E. Zahir, A. M. Chakravarty. “SDM propagation model for multiple channels using ray theory.” Proc. SPIE 7682, Photonic Microdevices/Microstructures for Sensing II, 76820V (2010);

[30] S. H. Murshid, R. Biswas, and A. M. Chakravarty. “CAD model for co-propagating spatially multiplexed channels of same wavelength over standard multimode fibers.” Proc. SPIE 7339 Enabling Photonics Technologies for Defense, Security, and Aerospace Applications V. (2009)

[31] Murshid, Syed H., Abhijit Chakravarty, and Raka Biswas. "CAD analysis of four co-propagating spatial domain multiplexed (SDM) channels of same wavelength in optical fibers." Frontiers in Optics. Optical Society of America, 2009.

[32] Murshid, Syed H., Abhijit Chakravarty, and Raka Biswas. "Simultaneous transmission of two channels operating at the same wavelength in standard multimode fibers." Quantum Electronics and Laser Science Conference. Optical Society of America, 2008.

[33] Murshid, Syed H., and Abhijit Chakravarty. "Dispersion model of two simultaneously propagating spatial domain multiplexing (SDM) channels of same wavelength in step index multimode fibers." Frontiers in Optics. Optical Society of America, 2009.

[34] Murshid, Syed H., Abhijit Chakravarty, and Raka Biswas. "Beam profile of two simultaneously propagating channels of same wavelength in step index multimode fibers." Frontiers in Optics. Optical Society of America, 2008.

[35] Murshid, Syed H., Abhijit Chakravarty, and Raka Biswas. "Attenuation model of spatially separated co-propagating optical channels of same wavelength in standard step index multimode fibers." Proceedings of the IASTED International Conference. Vol. 648. 2009.

[36] A. N. Alexeyev, T. A. Fadeyeva, A. V. Volyar. “Optical Vortices and the flow of their angular momentum in a multimode fiber.”, Semiconductor Physics, Quantum Electronics & Optoelectronics. 1998. V1, N1. P. 82-89.

[37] J. E. Curtis and D. G. Grier, “Structure of optical vortices,” Phys. Rev. Lett.90, 133901 (2003).